The Journal of Experimental Biology 213, 2582-2588

doi:10.1242/jeb.044271

On muscle, tendon and high heels

R. Csapo[1,2,*], C. N. Maganaris[1], O. R. Seynnes[1] and M. V. Narici[1]

[1]Institute for Biomedical Research into Human Movement and Health, Manchester Metropolitan University, Faculty of Science and Engineering, John Dalton Building, Chester Street, Manchester, M1 5GD, UK and [2]University of Vienna, Centre of Sport Sciences and University Sports, Department of Sports Medicine and Training Science, Auf der Schmelz 6, 1150 Vienna, Austria

*Author for correspondence (robert.csapo@univie.ac.at)

Accepted 26 April 2010

SUMMARY

Wearing high heels (HH) places the calf muscle–tendon unit (MTU) in a shortened position. As muscles and tendons are highly malleable tissues, chronic use of HH might induce structural and functional changes in the calf MTU. To test this hypothesis, 11 women regularly wearing HH and a control group of 9 women were recruited. Gastrocnemius medialis (GM) fascicle length, pennation angle and physiological cross-sectional area (PCSA), the Achilles' tendon (AT) length, cross-sectional area (CSA) and mechanical properties, and the plantarflexion torque–angle and torque–velocity relationships were assessed in both groups. Shorter GM fascicle lengths were observed in the HH group (49.6±5.7 mm *vs* 56.0±7.7 mm), resulting in greater tendon-to-fascicle length ratios. Also, because of greater AT CSA, AT stiffness was higher in the HH group (136.2±26.5 N mm^{-1} *vs* 111.3±20.2 N mm^{-1}). However, no differences in the GM PCSA to AT CSA ratio, torque–angle and torque–velocity relationships were found. We conclude that long-term use of high-heeled shoes induces shortening of the GM muscle fascicles and increases AT stiffness, reducing the ankle's active range of motion. Functionally, these two phenomena seem to counteract each other since no significant differences in static or dynamic torques were observed.

Key words: high heels, muscle architecture, muscle contraction, muscle plasticity, tendon mechanical properties, tendon plasticity.

INTRODUCTION

Skeletal muscle is a highly malleable tissue that can adapt both morphologically and functionally to chronic alterations in mechanical loading. Animal experiments performed in the early 1970s (Tabary et al., 1972; Williams and Goldspink, 1973) and later (Ohira et al., 2000) showed a loss of sarcomeres in series when muscles are immobilised in a shortened position. In humans, one common condition that places muscle–tendon units (MTUs) in a shortened position is high heel (HH) wearing. In this condition the length of the calf MTU is reduced by the ankle plantarflexion caused by the heel lift imposed by the HH. Contrary to the experimental conditions used for animal muscles, however, the calf MTU is not immobilised in women wearing HH but is rather coerced to temporarily operate at reduced length. But can this specific functional demand result in MTU adaptive responses? Herzog and colleagues (Herzog et al., 1991) compared the rectus femoris moment–length relationship of high-performance athletes engaged in different disciplines, who chronically use this muscle at distinctly different lengths, and found that runners were relatively stronger at longer muscle lengths and cyclists stronger at shorter muscle lengths. Although it is difficult to draw conclusions about the presence or lack of functional adaptations from a comparative study between different subjects, the finding of Herzog and colleagues (Herzog et al., 1991) supports the hypothesis that length-dependent adaptations may be provoked not only by immobilisation but also by habitual activity and the functional demands it imposes. The plasticity to changes in functional demands is shown not only by skeletal muscles but also by tendons. Being mechanosensitive tissues (Reeves et al., 2005; Rosager et al., 2002), tendons may adjust both their size and their material properties (Wren et al., 1998) to maintain constant strain when the forces acting on them increase or decrease. Consequently, any change in the contractile behaviour of the plantarflexor muscles induced by long-term use of HH might indirectly also affect tendon mechanical properties. Furthermore, a growing amount of evidence shows that HH wearing is associated with higher ground reaction forces (Ebbeling et al., 1994; Hong et al., 2005; Snow and Williams, 1994), indicating greater muscle and tendon forces, which may trigger tendon hypertrophy or improve its material properties. In the light of the above considerations, the present study aimed to investigate whether parameters of the calf MTU relevant to contractile force production would be modified by long-term use of high-heeled shoes. Specifically, we hypothesised that regular wearing of stilettos would lead to a shortening of the fascicles of the gastrocnemius muscle together with changes in the mechanical properties of the Achilles' tendon (AT), resulting in functional alterations, as seen in the torque–angle and torque–velocity relationships.

MATERIALS AND METHODS

Subjects

To test the above-mentioned hypotheses we approached female volunteers regularly wearing HH *via* posters and advertisements in the local media. To meet our criteria for inclusion, subjects had to have worn stilettos with a minimum heel height of 5 cm at least five times a week for a minimum of 2 years. Eventually, our study population consisted of 11 women (age 42.9±11.0 years; height 166.5±7.1 cm; mass 65.6±11.0 kg) regularly wearing high heels (HH group) and a control group (CTRL) of 9 women (age 33.2±9.3 years; height 170.2±5.8 cm; mass 64.4±6.3 kg). The differences in age, height and mass between groups were non-significant (P>0.05). The HH group reported that they wore HH for 60.7±20.7 h a week whereas the CTRL group commonly wore flat shoes (use of HH for 2.3±3.7 h a week). Because of time constraints, physical activity levels and habits could not be assessed. All measurements were carried out for the dominant leg only, defined as the leg preferentially used to regain balance when unexpectedly jostled. Participants gave written, informed consent to participate in the study, which was approved by the Ethics Committee of the Institute for Biomedical Research Into Human Movement and Health of the Manchester Metropolitan University.

Morphological measurements

Axial-plane magnetic resonance imaging (MRI) scans were performed along the length of the triceps surae muscle to measure the volumes of the gastrocnemius lateralis (GL), gastrocnemius medialis (GM) and soleus (SOL) muscle. Scans were acquired using an extremity coil-fixed 0.2 T MRI scanner (E-Scan, Esaote Biomedica, Genoa, Italy) with the following scanning parameters: turbo 3D T1-weighted sequence, slice thickness 6.3 mm, time to echo 16 ms, repetition time 38 ms, matrix 256×256 pixels, field of view 180 mm×180 mm.

AT moment arms (MA) were determined from sagittal-plane MRI scans of the ankle joint at an angle of 0 deg using a modified Reuleaux method (Reuleaux, 1875). This method assumes that the centre of rotation of the ankle corresponds to the midpoint of a circle fitted around the talus. The MA was defined as the perpendicular distance from the AT to the centre of rotation. MA images were obtained with the following scanning parameters: spin echo T1-weighted sequence, slice thickness 5 mm, time to echo 26 ms, repetition time 500 ms, matrix 256×256 pixels, field of view 200 mm×200 mm. The sagittal images were then resliced along the axial plane to measure tendon cross-sectional area (CSA). These measurements were obtained 3 cm proximal to the tendon's point of insertion on the calcaneus, which typically corresponds to the narrowest part of the tendon (Magnusson et al., 2003). All MRI images were processed and analysed using a publicly available DICOM file viewer (Osirix medical imaging software v.3.5.1, Osirix, Atlanta, GA, USA).

Muscle architecture

Fascicle length (L_f) and pennation angle (θ) were measured in the GM at midlength in the centre of the muscle belly using real-time B-mode ultrasonography with a 10 cm, 7.5 MHz linear array ultrasound probe (MyLab 70, Esaote Biomedica). Sagittal plane images were recorded at five different joint angles (–20 to +20 deg in steps of 10 deg) with the subjects lying prone on the examination bed of an isokinetic dynamometer, as described in 'Dynamometric measurements' below. To assess the test–retest reliability, two ultrasound scans were recorded at each joint angle and each ultrasound scan was analysed on two separate days. Intraclass correlation coefficients ranged from 0.94 to 0.99 for measurements of L_f and from 0.96 to 0.99 for measurements of θ. Furthermore, the validity of this ultrasound technique for the assessment of muscle architecture has previously been tested on human cadavers by us and others (Chleboun et al., 2001; Kawakami et al., 1993; Narici et al., 1996). The resting position of the ankle was defined as the joint angle coinciding with 0 N m of passive tension torque, as recorded during automated movement of the foot from a fully dorsiflexed to plantarflexed position. The resting L_f and resting θ represent the values corresponding to the resting position of the ankle. Values of L_f and θ were subsequently interpolated linearly (R^2=0.98) and the physiological cross-sectional area (PCSA) of the GM muscle was calculated as the ratio between GM volume and resting L_f.

Tendon mechanical properties

The structural stiffness (K) and Young's modulus (E) of the AT were examined by measuring the tendon elongation during an isometric ramp contraction, according to the principles previously described by Maganaris and colleagues (Maganaris, 2002; Maganaris and Paul, 2002). In brief, the ultrasound probe was placed over the distal myotendinous junction of the GM muscle in the sagittal plane. An external marker fixed to the skin, which cast a shadow on the ultrasound images, served as a reference position. The participants then conducted an isometric maximum voluntary plantarflexion contraction (MVC) at a joint angle of 0 deg as detailed in 'Dynamometric measurements' below. The displacement of the myotendinous junction induced by the muscular contraction was recorded during the entire contraction and measured by evaluating the ultrasound images corresponding to 0, 20, 40, 60, 80 and 100% of MVC. The images were analysed with publicly available imaging software (ImageJ 1.43b, NIH, Bethesda, MD, USA). To prevent overestimation of the tendon elongation due to unintentional joint rotation during isometric contraction (Arampatzis et al., 2008), the displacement of the myotendinous junction induced by passive motion of the foot was measured by sonography. The amount of erroneous joint rotation during isometric contraction was determined using an electrogoniometer (K100, Biometrics Ltd, Cwmfelinfach, UK) attached to the ankle. This allowed the correction of the tendon elongation data for ankle joint rotation.

The forces acting on the AT were estimated from the equation F=cTQ×MA^{-1}, where cTQ is the plantarflexion torque corrected for antagonistic coactivation and MA is the ankle moment arm determined by MRI as described in 'Morphological measurements' above. The force and corresponding tendon elongation data were fitted with second-order polynomials, which gave R^2 values between 0.97 and 0.98. The structural stiffness K (N mm^{-1}) is defined as the slope of the force–elongation curve in its linear region (Maganaris et al., 2008). To allow a valid comparative outcome of K between subjects, K must refer to the same force region and therefore it was calculated in the maximum 20% force region of the weakest subject (O'Brien et al., 2010), for whom the estimated maximum force was 878 N. Additionally, tendon stress (MPa) was computed by normalising the tendon forces to the tendon CSA as measured by MRI. Tendon strain is the ratio of tendon elongation over the tendon resting length, expressed as a percentage. Tendon length (L_{tend}) was defined as the length between the distal myotendinous junction and the tendon's insertion on the calcaneus. Young's modulus E (MPa), reflecting the intrinsic material properties of the tendon, was calculated as the product of stiffness and the tendon's length-to-CSA ratio.

Dynamometric measurements

The torque–angle characteristics of the plantarflexor muscles were assessed by a series of isometric MVCs using an isokinetic dynamometer (Cybex NORM, Cybex International, New York, NY, USA). Subjects were lying prone with their knees in the anatomical position and the foot of the tested (dominant) leg firmly strapped to the footplate of the dynamometer. The axis of rotation of the ankle, defined as the line connecting the two malleoli, was carefully aligned with the axis of rotation of the dynamometer. After a warm-up period consisting of five submaximal contractions, the participants were instructed to perform maximal plantarflexion and dorsiflexion contractions at joint angles of –20, –10, 0, 10 and 20 deg, where 0 deg represents a right angle between the axis of the foot and the lower leg, and positive values a plantarflexed and negative values a dorsiflexed joint position, respectively. The MVC was determined as the peak torque over a 5 s contraction. Verbal encouragement was given for additional motivation. To examine the relative production of force across the joint angular range, the angle-specific maximum torque values were normalised to each subject's greatest maximum isometric torque.

To obtain torque–velocity relationships, maximum isokinetic torque was recorded, after accounting for the torque oscillations due to the inertia of the limb-lever system (Perrine and Edgerton, 1978; Sapega et al., 1982), at the angular velocities of 0.87, 1.75, 2.62 and 3.49 rad s^{-1} (50, 100, 150 and 200 deg s^{-1}), which were distributed in a randomised order. At 3.49 rad s^{-1}, some participants were unable to reach the preset angular velocity, so only the data from the three lower test velocities could be considered for further analysis. The range of motion was preset from –20 to +20 deg. After a familiarisation trial, subjects performed three consecutive contractions at each angular velocity with at least 2 min rest between bouts. Torque and joint angle were recorded simultaneously using an external analog-to-digital converter (Biopac MP100, Biopac Systems, Santa Barbara, CA, USA). The experimental torque–velocity values were then fitted (R^2=0.99 for both HH and CTRL) using the exponential equation: $v=(e^{-P/b}-e^{-P0/b})a$, where v is the angular velocity (rad s^{-1}), P is torque (N m), P_0 represents the maximal isometric torque (MVC), and a and b are experimentally determined constants. This equation has been shown to be most applicable to torque–velocity data measured *in vivo* (Thomas et al., 1987). The mean values of the constants were a=14.46, b=24.50 in the HH group and a=13.83, b=22.42 in the CTRL group. Based on the resulting fitted torque–velocity curves, power was calculated as the product of angular velocity (rad s^{-1}) and torque (N m). The torque–velocity curves were then normalised to the GM L_f of the respective participants, to account for differences in L_f and thus the number of sarcomeres in series. For simple dimensional purposes, the values in rad s^{-1} were multiplied by 16.0, a conversion factor published by Wickiewicz and colleagues (Wickiewicz et al., 1984) used to transform angular velocities (rad s^{-1}) into linear velocities (mm s^{-1}).

To correct the plantarflexion torque values for antagonistic coactivation, electromyographic activity on the tibialis anterior muscle (TA) was recorded during both plantarflexion and dorsiflexion MVCs. After reducing the skin impedance below 5 kΩ by standard preparation including shaving, gentle abrasion and cleaning with an alcohol-based tissue pad, two bipolar Ag–AgCl surface electrodes (10 mm inter-electrode distance) were placed in the central region of the TA, along the muscle's sagittal axis. An additional reference electrode was placed over the patella. The raw EMG data were digitised (sampling frequency of 2 kHz), band-pass filtered between 50 and 500 Hz, rectified and integrated over 500 ms around the peak torque using commercially available software (Acqknowledge, Biopac Systems). Assuming a linear relationship between EMG level and torque, the TA's EMG activity during plantarflexion was used to estimate the corresponding antagonistic torque (Maganaris et al., 1998).

Data analysis

Differences between groups were tested either with mixed-factorial ANOVAs or, where appropriate, with independent sample t-tests. The statistical level of significance was set at P<0.05 and values are reported as means ± s.d.

RESULTS

Morphological measurements

No significant differences in GM, GL and SOL muscle volumes were observed between the HH and CTRL groups. Likewise, GM PCSA, L_{tend} and AT MA were similar in the two groups. Tendon CSA was significantly greater in the HH group, but the GM PCSA:AT CSA ratio was similar (P>0.05) in the two groups. Also, the resting position of the ankle was found to be significantly more plantarflexed in the HH group. All measurements of morphological parameters and muscle architecture are summarised in Table 1.

In both groups, GM L_f increased from 47.7±6.8 mm as measured at a joint angle of +20 deg to 67.07±7.18 mm (–20 deg), whereas θ decreased from 20.23±2.11 deg (+20 deg) to 15.00±1.53 deg (–20 deg). In agreement with the more plantarflexed resting position of the ankle, resting L_f was significantly shorter in the HH group. No significant differences in resting θ were found. GM PCSA was greater by 8.4% in the HH group; however this did not reach statistical significance.

As a consequence of the shorter resting L_f, the tendon-to-fascicle length ratio tended to be greater in the HH group (HH 3.86±0.53; CTRL 3.38±0.48; P=0.051). Likewise, the amount of fascicle shortening induced by passive joint rotation (Fig. 1) was greater in the HH group (F=5.308, d.f.=1, P<0.05). *Post-hoc* independent sample t-tests revealed that the change in L_f caused by a 30 deg rotation of the foot (–20 to +10 deg) differed significantly (P<0.05).

Tendon mechanical properties

Force–elongation curves for the HH and CTRL group tendons followed different patterns (Fig. 2).

Tendon stiffness K was found to be significantly greater in the HH group (HH 136.2±26.5 N mm^{-1}; CTRL 111.3±20.2 N mm^{-1};

Table 1. Morphological measurements and muscle architecture

Characteristics	HH group (N=11)		CTRL group (N=9)		P-value
	Mean	s.d.	Mean	s.d.	
GM volume (cm^3)	199.06	51.57	206.28	44.34	0.744
GL volume (cm^3)	107.36	14.02	113.40	13.41	0.341
SOL volume (cm^3)	390.72	85.77	411.16	64.75	0.563
Resting L_f (mm)	49.60	5.71	55.99	7.71	0.047
Resting θ (deg)	18.48	1.50	18.84	1.33	0.587
GM PCSA (cm^2)	40.06	9.36	36.71	4.86	0.345
L_{tend} (cm)	18.91	1.29	18.69	1.71	0.746
Tendon CSA (mm^2)	53.99	4.46	50.54	2.17	0.049
Tendon MA (mm)	48.41	4.26	47.00	2.92	0.407
Resting ankle position (deg)	11.42	1.95	6.32	2.38	0.000
L_{tend}:L_f	3.86	0.53	3.38	0.48	0.051
GM PCSA:tendon CSA	74.60	17.40	72.95	11.67	0.803

HH, high heels; CTRL, control; GM, gastrocnemius medialis muscle; GL, gastrocnemius lateralis muscle; SOL, soleus muscle; L_f, fascicle length; θ, pennation angle; PCSA, physiological cross-sectional area; L_{tend}, tendon length; CSA, cross-sectional area; MA, moment arm.

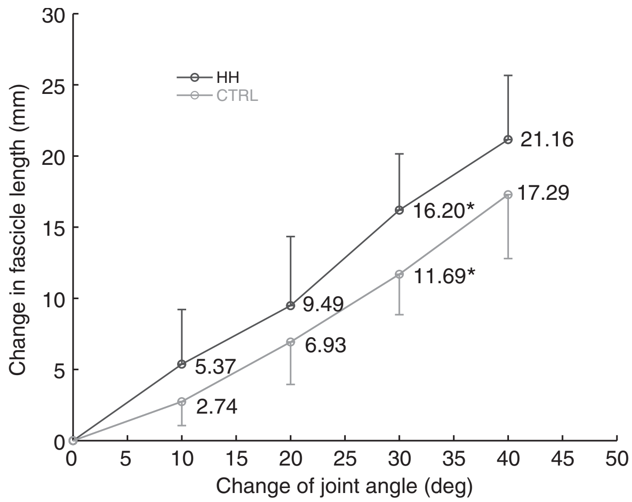

Fig. 1. Changes in fascicle length L_f induced by passive joint rotation. *High heel (HH) and control (CTRL) group values are significantly different at $P<0.05$.

$P<0.05$), but no significant differences in E (HH 471.19±94.76 MPa; CTRL 417.43±85.09 MPa; P=0.203) were observed. The greater K in the HH group was due to differences in tendon dimensions (tendon CSA approximately 7% greater in HH) rather than to tendon length or tendon material properties.

Maximum tendon stress was insignificantly greater in the HH group (HH 33.25±8.48 MPa; CTRL 30.07±8.76 MPa). However, differences in maximum strain were found to be significant (HH 5.74±1.19%; CTRL 6.98±1.00%; $P<0.05$). The stress–strain curves for the HH and CTRL groups are displayed in Fig. 3.

Dynamometric measurements

Torque–angle relationship

The plantarflexion torque–angle relationships for both groups are shown in Fig. 4.

The HH group achieved greater torques at all joint positions, yet the observed differences between groups were non-significant. After normalisation to maximum torque, the torque–angle profiles followed largely congruent patterns (Fig. 5).

Torque–velocity relationship

The torque–velocity relationship was not statistically different between groups. This holds true for the data expressed in absolute terms (Fig. 6) or normalised to L_f (Fig. 7). Also, peak power and the related optimal contraction velocity (v_{opt}) were found to be similar in the two groups.

DISCUSSION

The aim of the present study was to investigate the effects of chronic use of HH on the anatomical and functional properties of the calf MTU. Our findings show that long-term use of HH shoes leads to a shortening of the gastrocnemius muscle fascicles together with an increase in AT size and stiffness.

In line with the reduced GM L_f, we observed tendon-to-fascicle length ratios that were ~14% greater in the HH group. This ratio is used to predict the amount of fascicle shortening during isometric contraction (Zajac, 1989), as it reflects the compliance of the MTU and thus the degree of sarcomere shortening (Ito et al., 1998). Consequently, we expected the finding of greater tendon-to-fascicle length ratios in the HH group to be reflected in a right-shift of the normalised torque–angle relationship, i.e. peak torques would be achieved at longer MTU lengths. Yet, in contrast with this hypothesis and with the findings reported by Herzog and colleagues (Herzog et al., 1991), very similar relative torque–angle relationships were found in the two groups; this suggests that the effects of the altered tendon-to-fascicle length ratio (right-shift) are compensated for by the increased tendon stiffness (left-shift) in the HH group.

Just as under isometric conditions, isokinetic torque and power values were similar in the two groups. The muscle force generated in dynamic contractions is known to be affected by both the muscle's PCSA, reflecting the total number of sarcomeres in parallel, and L_f, affecting the length–force relationship of the muscle (Lieber and Friden, 2000; Narici, 1999). As GM L_f was shorter in the HH group, we expected this finding to be reflected by lower torque–velocity curves in this group, particularly for values of maximum contraction velocity v_{max}, which is known to be dependent on the number of

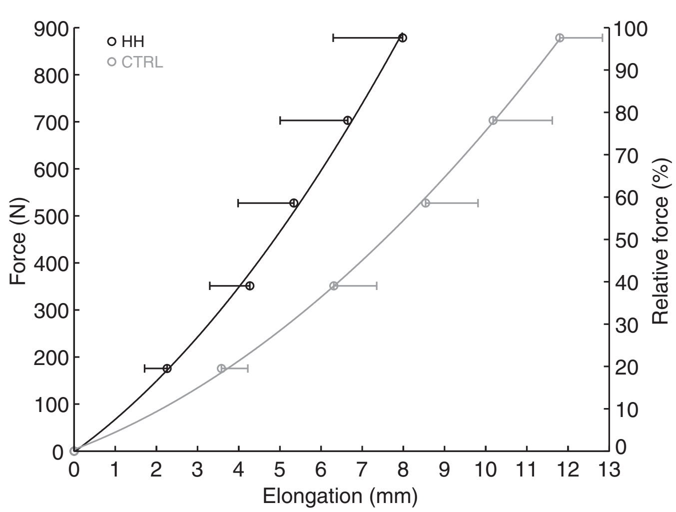

Fig. 2. Tendon force–elongation relationship. Elongation data are normalised to 878 N. Values are presented as means ± s.d.

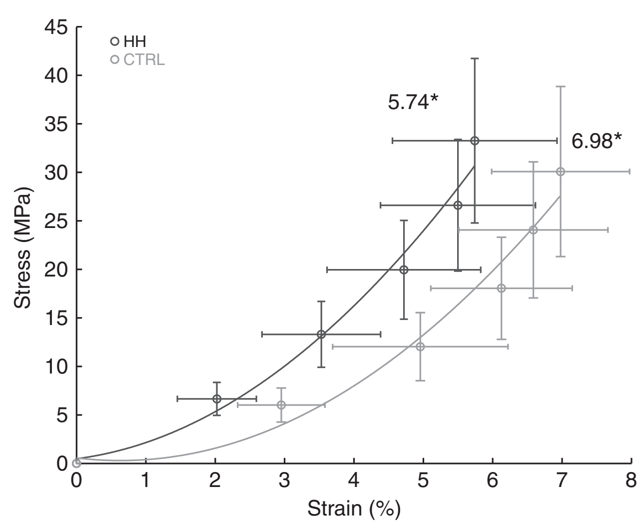

Fig. 3. Tendon stress–strain relationship. Values are presented as means ± s.d. *Maximum tendon strain values of the HH and CTRL groups are significantly different at $P<0.05$.

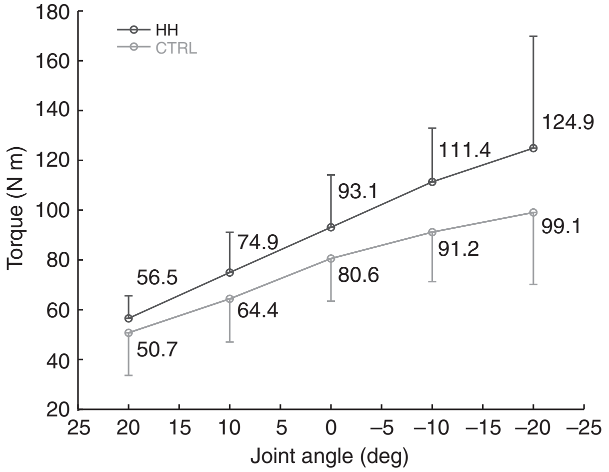

Fig. 4. Torque–angle relationship. Values are presented as means ± s.d.

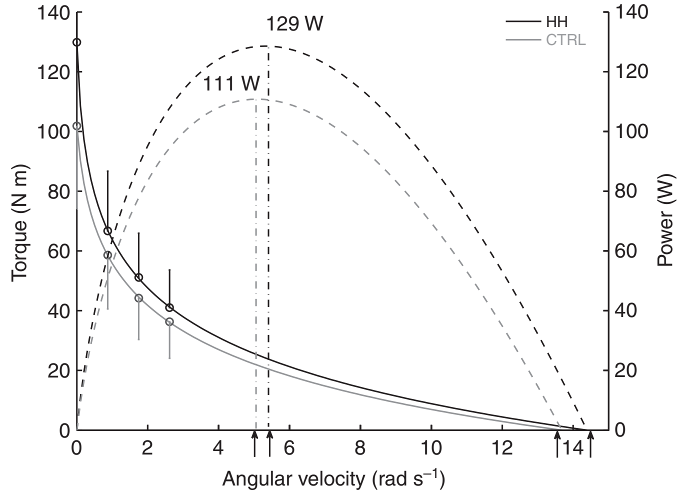

Fig. 6. Torque–velocity and power–velocity relationships. The experimental values (open circles) were fitted using the exponential equation $v=(e^{-P/b}-e^{P0/b})a$. Values are presented as means ± s.d. Arrows indicate the estimated optimal contraction velocity v_{opt} (HH 5.3 rad s^{-1}; CTRL 5.1 rad s^{-1}) and maximum contraction velocity v_{max} (HH 14.4 rad s^{-1}; CTRL 13.7 rad s^{-1}).

sarcomeres in series, and thus on L_f. The lack of difference in performance in dynamic contractions may be attributed either to differences in PCSA or to the alterations in the tendon-to-fascicle length ratio. It is known that relatively longer tendons can account for a greater part of the motion of the entire MTU (Roberts, 2002; Roberts et al., 1997), allowing the fascicles to shorten at a slower speed and thus operate in a more advantageous region of the force–velocity curve. Therefore it seems that, as for isometric contractions, the morphological changes of the calf MTU induced by long-term use of HH do not impair dynamic torque production.

The AT hypertrophy, and the related increase in the stiffness of the tendon–aponeurosis complex observed in the HH group, agree well with the finding of greater angles of ankle plantarflexion at rest in the HH group and the greater change in L_f induced by passive joint rotation. This is because with stiffer tendons the fascicles would be forced to alter their length more for a given change in MTU length. Thus the present results suggest that shorter L_f and increased tendon stiffness both contribute to the reduction in the ankle active range of motion. This may also explain the muscular discomfort that women regularly walking in HH report experiencing when walking in flat shoes (Opila et al., 1988). A possible reason for the increase in AT size and stiffness may be that the muscle forces acting on the tendon–aponeurosis complex are relatively greater in the HH group. Although the differences in GM PCSA were not statistically significant, the similar PCSA-to-tendon CSA ratios observed in the two groups confirm the notion that the size of the tendon adapts to the muscle forces exerted on it (Cutts et al., 1991). This trend towards plantarflexor hypertrophy in habitual HH wearers may represent an adaptive response to the overloading imposed on the muscles during HH gait. Indeed, when walking on HH, the body's centre of mass is raised and shifted forward (Ebbeling et al., 1994; Snow and Williams, 1994). This might force the plantarflexors to generate higher torques

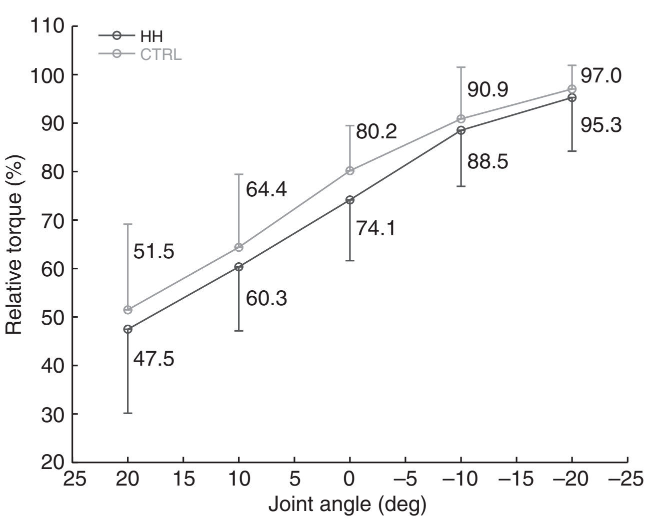

Fig. 5. Relative torque–angle relationship. Values are presented as means ± s.d.

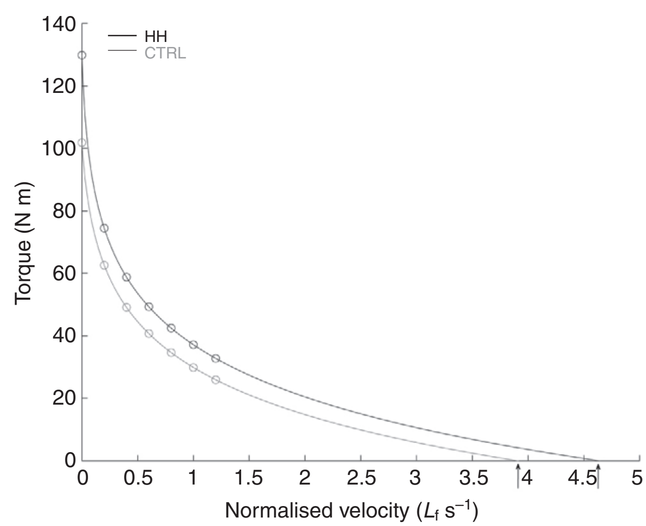

Fig. 7. Torque–velocity relationships after normalisation to GM L_f. Arrows indicate the estimated v_{max} (HH 4.64 L_f s^{-1}; CTRL 3.91 L_f s^{-1}).

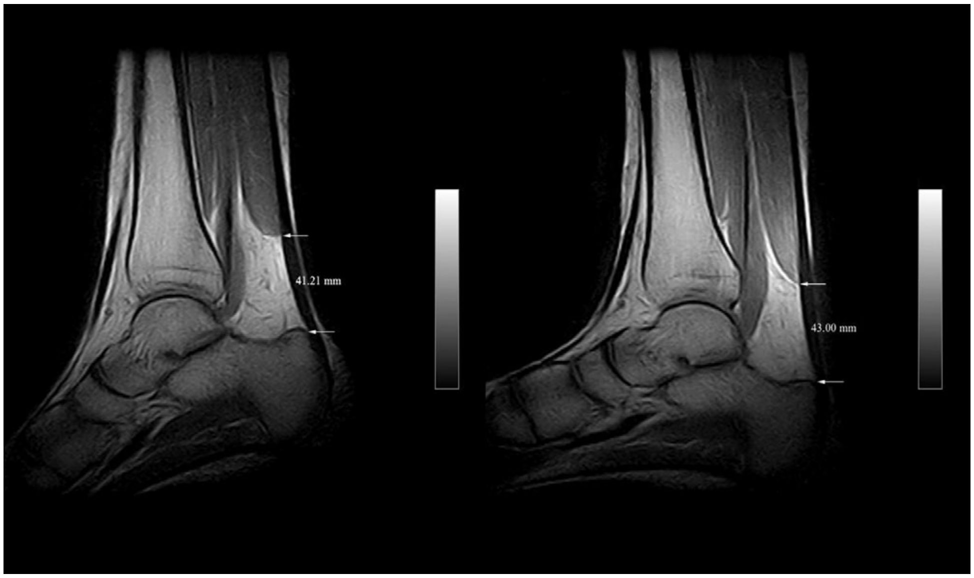

Fig. 8. Sagittal MRI scan of the plantarflexor muscle–tendon unit (MTU). Images show the MTU while standing on a wooden wedge (left) and on a flat surface (right). Both images were obtained from a non-habitual HH wearer.

for take-off during locomotion and, possibly, to counter the destabilizing effects caused by the altered ground reaction force vector (Murnaghan et al., 2009), eventually promoting an increase in tendon CSA, and a similar trend towards muscle hypertrophy. Also, ground reaction forces, reflecting contractile forces, are reported to increase as a function of heel height (Ebbeling et al., 1994; Hong et al., 2005; Yung-Hui and Wei-Hsien, 2005). Findings of increased calf electromyographic activity with greater heel height (Stefanyshyn et al., 2000) further substantiate the hypothesis of overload-induced tendon hypertrophy in habitual HH wearers.

GM fascicles were shorter by approximately 13% in the HH group. This loss of in-series sarcomeres might represent the muscle's adaptation to chronically being forced to operate in a shortened position (Herzog et al., 1991). Indeed, high-heeled shoes lift the heels by several centimetres and place the plantarflexor MTU at a considerably shorter length. In women only occasionally wearing HH, this change of joint position presumably increases the tendon slack (see Fig. 8).

As adequate levels of tension within the MTU are required for both effective force transmission to the skeleton and proprioception (Cronin et al., 2008), the plantarflexor muscles might acutely react by increasing their tonic activity to take up the excessive tendon slack. Putting on HH might therefore cause excessive sarcomere overlap, forcing muscle fascicles to operate in a disadvantageous region of their length–tension curve. The reduction of L_f observed in regular HH wearers may therefore represent a long-term adaptation of the plantarflexor muscles aimed at resetting a normal sarcomere operating range. Additionally, the greater stiffness of the tendon–aponeurosis complex seen in the HH group may contribute to the maintenance of MTU tension and therefore be beneficial for force transmission and proprioception when wearing HH shoes.

In conclusion, we observed shortened gastrocnemius L_f and increased AT stiffness in habitual HH wearers, which might reduce the ankle active range of motion and thus explain the discomfort these women experience when walking in flat shoes. These results strongly support the hypothesis that muscle structure may adapt to a chronic change in functional demand. Functionally, the observed MTU adaptations seem to compensate for each other since no significant differences in torque–angle and torque–velocity relationships were observed between the HH and CTRL group women.

LIST OF SYMBOLS AND ABBREVIATIONS

AT	Achilles' tendon
CSA	cross-sectional area
CTRL	control
E	Young's modulus
GL	gastrocnemius lateralis muscle
GM	gastrocnemius medialis muscle
HH	high heels
K	tendon stiffness
L_f	fascicle length
L_{tend}	tendon length
MA	moment arm
MRI	magnetic resonance imaging
MTU	muscle–tendon unit
MVC	maximum voluntary contraction
PCSA	physiological cross-sectional area
SOL	soleus muscle
TA	tibialis anterior muscle
v_{max}	maximum contraction velocity
v_{opt}	optimal contraction velocity
θ	pennation angle

ACKNOWLEDGEMENTS

We thank all of our volunteers for their kind contribution to the study and Mr Martino Franchi for his assistance with data acquistion.

REFERENCES

Arampatzis, A., Monte, G. D. and Karamanidis, K. (2008). Effect of joint rotation correction when measuring elongation of the gastrocnemius medialis tendon and aponeurosis. *J. Electromyogr. Kinesiol.* **18**, 503-508.
Chleboun, G. S., France, A. R., Crill, M. T., Braddock, H. K. and Howell, J. N. (2001). In vivo measurement of fascicle length and pennation angle of the human biceps femoris muscle. *Cells Tissues Organs* **169**, 401-409.
Cronin, N. J., Peltonen, J., Ishikawa, M., Komi, P. V., Avela, J., Sinkjaer, T. and Voigt, M. (2008). Effects of contraction intensity on muscle fascicle and stretch reflex behavior in the human triceps surae. *J. Appl. Physiol.* **105**, 226-232.
Cutts, A., Alexander, R. M. and Ker, R. F. (1991). Ratios of cross-sectional areas of muscles and their tendons in a healthy human forearm. *J. Anat.* **176**, 133-137.
Ebbeling, C. J., Hamill, J. and Crussemeyer, J. A. (1994). Lower extremity mechanics and energy cost of walking in high-heeled shoes. *J. Orthop. Sports Phys. Ther.* **19**, 190-196.
Herzog, W., Guimaraes, A. C., Anton, M. G. and Carter-Erdman, K. A. (1991). Moment–length relations of rectus femoris muscles of speed skaters/cyclists and runners. *Med. Sci. Sports Exerc.* **23**, 1289-1296.
Hong, W. H., Lee, Y. H., Chen, H. C., Pei, Y. C. and Wu, C. Y. (2005). Influence of heel height and shoe insert on comfort perception and biomechanical performance of young female adults during walking. *Foot Ankle Int.* **26**, 1042-1048.
Ito, M., Kawakami, Y., Ichinose, Y., Fukashiro, S. and Fukunaga, T. (1998). Nonisometric behavior of fascicles during isometric contractions of a human muscle. *J. Appl. Physiol.* **85**, 1230-1235.
Kawakami, Y., Abe, T. and Fukunaga, T. (1993). Muscle-fiber pennation angles are greater in hypertrophied than in normal muscles. *J. Appl. Physiol.* **74**, 2740-2744.

Lieber, R. L. and Friden, J. (2000). Functional and clinical significance of skeletal muscle architecture. *Muscle Nerve* **23**, 1647-1666.
Maganaris, C. N. (2002). Tensile properties of in vivo human tendinous tissue. *J. Biomech.* **35**, 1019-1027.
Maganaris, C. N. and Paul, J. P. (2002). Tensile properties of the in vivo human gastrocnemius tendon. *J. Biomech.* **35**, 1639-1646.
Maganaris, C. N., Baltzopoulos, V. and Sargeant, A. J. (1998). Differences in human antagonistic ankle dorsiflexor coactivation between legs; can they explain the moment deficit in the weaker plantarflexor leg? *Exp. Physiol.* **83**, 843-855.
Maganaris, C. N., Narici, M. V. and Maffulli, N. (2008). Biomechanics of the Achilles tendon. *Disabil. Rehabil.* **30**, 1542-1547.
Magnusson, S. P., Beyer, N., Abrahamsen, H., Aagaard, P., Neergaard, K. and Kjaer, M. (2003). Increased cross-sectional area and reduced tensile stress of the Achilles tendon in elderly compared with young women. *J. Gerontol. A Biol. Sci. Med. Sci.* **58**, 123-127.
Murnaghan, C. D., Elston, B., Mackey, D. C. and Robinovitch, S. N. (2009). Modeling of postural stability borders during heel-toe rocking. *Gait Posture* **30**, 161-167.
Narici, M. V. (1999). Human skeletal muscle architecture studied in vivo by non-invasive imaging techniques: functional significance and applications. *J. Electromyogr. Kinesiol.* **9**, 97-103.
Narici, M. V., Binzoni, T., Hiltbrand, E., Fasel, J., Terrier, F. and Cerretelli, P. (1996). In vivo human gastrocnemius architecture with changing joint angle at rest and during graded isometric contraction. *J. Physiol.* **496**, 287-297.
O'Brien, T. D., Reeves, N. D., Baltzopoulos, V., Jones, D. A. and Maganaris, C. N. (2010). Mechanical properties of the patellar tendon in adults and children. *J. Biomech.* **43**, 1190-1195.
Ohira, Y., Yoshinaga, T., Wataru, Y., Ohara, M. and Takato, T. (2000). Effects of hindlimb suspension with stretched or shortened muscle length on contractile properties of rat solues. *J. Appl. Biomech.* **16**, 80-87.
Opila, K. A., Wagner, S. S., Schiowitz, S. and Chen, J. (1988). Postural alignment in barefoot and high-heeled stance. *Spine* **13**, 542-547.
Perrine, J. J. and Edgerton, V. R. (1978). Muscle force-velocity and power-velocity relationships under isokinetic loading. *Med. Sci. Sports* **10**, 159-166.
Reeves, N. D., Maganaris, C. N., Ferretti, G. and Narici, M. V. (2005). Influence of 90-day simulated microgravity on human tendon mechanical properties and the effect of resistive countermeasures. *J. Appl. Physiol.* **98**, 2278-2286.
Reuleaux, F. (1875). *Theoretische Kinematik: Grundzüge einer Theorie des Mas*chinenwesens. Braunschweig: F. Vieweg und Sohn.
Roberts, T. J. (2002). The integrated function of muscles and tendons during locomotion. *Comp. Biochem. Physiol. A Physiol.* **133**, 1087-1099.
Roberts, T. J., Marsh, R. L., Weyand, P. G. and Taylor, C. R. (1997). Muscular force in running turkeys: the economy of minimizing work. *Science* **275**, 1113-1115.
Rosager, S., Aagaard, P., Dyhre-Poulsen, P., Neergaard, K., Kjaer, M. and Magnusson, S. P. (2002). Load-displacement properties of the human triceps surae aponeurosis and tendon in runners and non-runners. *Scand. J. Med. Sci. Sports* **12**, 90-98.
Sapega, A. A., Nicholas, J. A., Sokolow, D. and Saraniti, A. (1982). The nature of torque "overshoot" in Cybex isokinetic dynamometry. *Med. Sci. Sports Exerc.* **14**, 368-375.
Snow, R. E. and Williams, K. R. (1994). High heeled shoes: their effect on center of mass position, posture, three-dimensional kinematics, rearfoot motion, and ground reaction forces. *Arch. Phys. Med. Rehabil.* **75**, 568-576.
Stefanyshyn, D. J., Nigg, B. M., Fisher, V., O'Flynn, B. and Liu, W. (2000). The influence of high heeled shoes on kinematics, kinetics, and muscle EMG of normal female gait. *J. Appl. Biomech.* **16**, 309-319.
Tabary, J. C., Tabary, C., Tardieu, C., Tardieu, G. and Goldspink, G. (1972). Physiological and structural changes in the cat's soleus muscle due to immobilization at different lengths by plaster casts. *J. Physiol.* **224**, 231-244.
Thomas, D. O., White, M. J., Sagar, G. and Davies, C. T. (1987). Electrically evoked isokinetic plantar flexor torque in males. *J. Appl. Physiol.* **63**, 1499-1503.
Wickiewicz, T. L., Roy, R. R., Powell, P. L., Perrine, J. J. and Edgerton, V. R. (1984). Muscle architecture and force–velocity relationships in humans. *J. Appl. Physiol.* **57**, 435-443.
Williams, P. E. and Goldspink, G. (1973). The effect of immobilization on the longitudinal growth of striated muscle fibres. *J. Anat.* **116**, 45-55.
Wren, T. A., Beaupre, G. S. and Carter, D. R. (1998). A model for loading-dependent growth, development, and adaptation of tendons and ligaments. *J. Biomech.* **31**, 107-114.
Yung-Hui, L. and Wei-Hsien, H. (2005). Effects of shoe inserts and heel height on foot pressure, impact force, and perceived comfort during walking. *Appl. Ergon.* **36**, 355-362.
Zajac, F. E. (1989). Muscle and tendon: properties, models, scaling, and application to biomechanics and motor control. *Crit. Rev. Biomed. Eng.* **17**, 359-411.